MDPI

Review

Independent Component Analyses Applied On Pulsed Thermographic Data For CFRP Inspection A Review

Julien Fleuret [1,‡*], Samira Ebrahimi [1,‡], Clemente Ibarra-Castanedo [1], and Xavier Maldague [1]

[1] Computer Vision and Systems Laboratory (CVSL), Department of Electrical and Computer Engineering, Laval University, Quebec City, QC G1V 0A6, Canada; jufle7 at ulaval.ca (J.F.)
* Correspondence: jufle7 at ulaval.ca
‡ These authors contributed equally to this work.

Abstract: In this study, we investigated the application of several ICA implementations for material inspection using pulsed thermography. We compared our results with state-of-the-art methods, PCT and PPT. We conducted our experiments on a reference CFRP sample. We evaluated the different algorithms for all the defects surfaces at a given depth and all the depth for a given defect surface. Our results show that ICA does not outperform PCT or PPT but provides similar results and follows the same trends, making it an approach of interest for further analysis on other materials. We also found that the different implementations of the ICA provide similar results, and no implementation significantly outperforms the other. Further investigations on noisy data and different materials are still needed to assess the interest of the ICA for material inspection. With that in mind, we also only investigated the unsupervised implementation of the ICA; therefore, some investigation of the supervised version of the ICA might still outperform the state-of-the-art approaches.

Keywords: ICA, ICT, PPT, PCT, CFRP

Citation: Fleuret, J.; Ebrahimi, S.; Ibarra-Castanedo, C., Maldague, X. Title. *Journal Not Specified* **2021**, *1*, 0. https://doi.org/

Received:
Accepted:
Published:

Publisher's Note: MDPI stays neutral with regard to jurisdictional claims in published maps and institutional affiliations.

Copyright: © 2021 by the authors. Submitted to *Journal Not Specified* for possible open access publication under the terms and conditions of the Creative Commons Attribution (CC BY) license (https://creativecommons.org/licenses/by/4.0/).

1. Introduction

Non Destructive Testing (NDT) is a very popular field in many fields of industry. Among the many different NDT fields, InfraRed Thermography (IRT) is a famous field for evaluating materials. IRT's approaches consist of a set of tomographic approaches that are helpful to assess a wide range of features, from material homogeneity to the presence of void or foreign materials within another material. Within the field of IR-NDT, Pulsed Thermography (PT) is a very famous method. Among its fame are its simplicity and ability to provide valuable results on a wide range of materials. PT consists of submitting a sample of interest to a pulse of energy. Once the pulse reaches the material, it becomes a thermal wave that propagates by conduction through the material. The propagation will be affected by many features such as non-homogeneity in the density of the material, crack, void, foreign material, to cite a few. A thermal camera then records the decay of temperature. Thermal cameras are well known for being sensitive to a wide range of phenomenon and noises, including some created by the device itself, resulting in a wide range of distortions during the creation of the data [1–5]. The literature offers many methods proposed to enhance and improve the data returned by the thermal camera during PT experiments. Among the most famous are the Pulsed Phase Thermography (PPT) [6] and the Principal Component Thermography (PCT) [7]. The former consists of transforming the sequence into the Fourier domain and analyze the phase. The latter consists of applying a PCA to the sequence to extract the most meaningful frames. PCA projects the sequence into an orthogonal domain while maximizing the variance of the projected data. Nonetheless, the PCA is well-known to be sensitive to the noise present in the data. Several improvements of the PCA have been proposed in the literature and successfully applied to PT data. Yousefi et al. [8] proposed to use

an improved version of the Candid Covariance-free Incremental Principal Component Analysis (CCIPCA) [9] under the name CCIPCT (Candid Covariance-free Incremental Principal Component Thermography). In their work, Yousefi et al. also update the cost function using the one proposed by Kompella et al. [10]. Later Yousefi et al. have proposed to apply the Sparse Principal Component Analysis (SPCA) [11] due to its increased robustness, under the name SPCT (Sparse Principal Component Thermography) [12]. SPCA robustness is mainly due to a penalization model called Least Absolute Shrinkage and Selection Operator or LASSO [13].

Another approach exists regarding the components analysis, among them the Independent Component Analysis (ICA) [14]. ICA, like PCA, tries to identify the most meaningful basis to project a multivariate dataset from a mathematical space to another. PCA uses an orthogonal transformation to convert a set of observations that may be correlated into a set of linearly uncorrelated variables. This set of uncorrelated variables is called the principal components. The ICA attempts to decompose the dataset as a set of independent signals. It is often used for blind signal separation. From a more formal point of view, the ICA assumes that the thermal camera data are a mixture of different signals.

$$\mathbf{x} = \mathbf{A}\mathbf{s} \tag{1}$$

From the PT point of view, we assume that each defect within a sample is an independent signal $\mathbf{s}$ mixed with another non-defective part of the sample. The matrix $\mathbf{A}$ is a square invertible matrix. The goal of the ICA algorithm is to find an estimation of $\mathbf{s}$ from the data $\mathbf{x}$ by computing $\mathbf{W} = \mathbf{A}^{-1}$.

$$\hat{\mathbf{s}} = \mathbf{W}\mathbf{x} \tag{2}$$

The matrix $\mathbf{W}$ is known in the literature as an unmixing matrix. As one can note in equation 1, ICA is an under-constrained problem. This problem is known as blind source separation. A main concept regarding the ICA is the measurement of the independence of the components, which is similar to measure the non-gaussianity of two samples. Several methods have been proposed in the literature over time [15,16]. Among the most famous is the work of Bell et al. [17], which was later extended by Lee et al. [18]. These works use the maximization of the output entropy of a neural network with non-linear outputs. Hyvärinen et al. [19] proposed a maximum likelihood approach, which at that time outperforms in terms of computation time the existing approaches. Recently Ablin et al. [20,21] proposed several approaches regarding the computation of the Hessian matrix within optimization algorithms. ICA approaches have been used in different approaches regarding IRNDT. Morabito et al. [22,23] were among the first to use ICA with Eddy-Current Testing (ECT) initially to analyze their features and later to detect and segment defects. Shin et al. [24] also used ICA to identify defects from an ECT distorted signal. Yang et al. [25] investigated the ICA application for defect detection in Pulsed Eddy-Current (PEC), which was later improved by Cheng et al. [26]. Wang et al. [27] used the method proposed by Hyvärinen et al. on Pulsed Thermographic data for the inspection of high silicon-oxygen phenolic resin. Javier-Rengifo et al. [28] already made a study regarding the application of both PCA and ICA in order to find a defect in Carbon Fiber Reinforced Polymer (CFRP) material. In their work, Javier-Renfigo et al. also proposed a new approach to select the best components for the ICA for applications regarding CFRP material inspection. However regarding the ICA method used in this study only investigated the method proposed by Hyvärinen et al. [19]. This paper investigates the usage of several state-of-the-art ICA methods on PT data for Carbon Fiber Reinforced Plastic (CFRP) inspection.

The rest of this paper is structured as follows. In the next section, the Independent Component Analysis is briefly introduced. Section 2, describes the different aspects of the experiments we conducted. Section 3 introduces the different results we generated from our experiments. Section 4 discuss and analyze the results. Finally, Section 5 concludes this work.

2. Materials and Methods

Our study aims to evaluate the accuracy of different formulations of the ICA on PT data and compare their results with state-of-the-art approaches. In this section, we introduce the different aspects of the experiments we conducted.

2.1. Data

In order to evaluate the potential interest of ICA in IRNDT, we analyzed a reference Carbon Fiber Reinforced Plastic (CFRP) sample. This sample contains twenty-five Teflon inserts which are divided into five batches of five defects. Each batch has five inserts having the same depth but different sizes (from 3x3 mm^2 to 15x15 mm^2). As illustrated in figure 1, each batch has been positioned at a specific depth (from 0.2 to 1 mm). The materials have been evaluated under a classic pulse thermographic procedure.

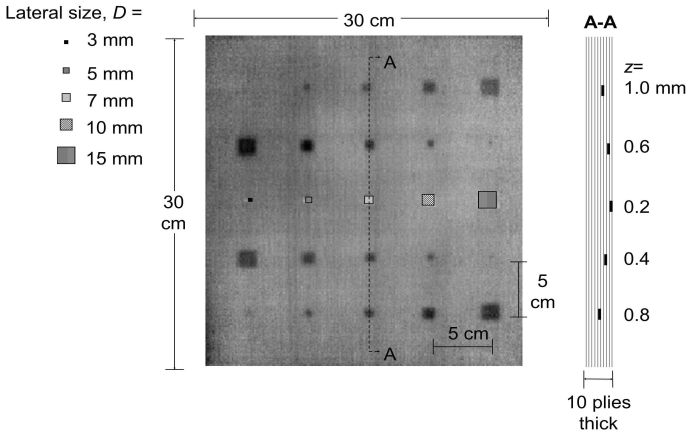

Figure 1. CFRP sample used for the experiments.

Each material has been stimulated from the front side by a pulse generated by two photographic flashes (Balcar FX 60, 5 ms thermal pulse, 6.4 $kJ/flash$). A mid-wave infrared (MWIR) camera FLIR x6900sc (1.5 μm to 5.0 μm, 14 bit per pixel, 640 $\times$ 512) was used for data acquisition. We conducted two acquisitions at different frequencies of acquisition. We acquired some data at a frequency of 145 Hz (145 images per second) and 120 Hz. For each experiment, a sequence between 2000 frames and 2200 frames was acquired during a period of 30 seconds. That duration ensured that the sensor had acquired both the warm-up and the cool-down.

2.2. Analysis

To evaluate the different implementations of the ICA, we chose two state-of-the-art methods, the Pulsed Phase Thermography [6] and the Principal Component Thermography [7]. Among the different formulation of the ICA, we investigated the ICA using Infor-Max [17], The ICA using Info-Max extended [18], the Fast-ICA [19], simple quasi newton ICA, and trusted region ICA, which were introduced by Albin et al. [20,21]. We also evaluated more recent approaches such as the uwedgeICA introduce [29] and the BIO-NICA [30]. For each frequency, we acquired a sequence of T images of dimensions $M \times N$ pixels. The first step consists of creating an overlay matrix of dimension $T \times P$ where $P = M.N$. T is the number of frames acquired in each sequence, P is the total number of pixels. Before applying the different algorithms we selected on the data overlay matrix we first standardize the content of it by centering to 0 and normalizing the standard deviation to 1. Once the ICA models are applied, we only keep the seven first components before reconstructing an output sequence. Because we choose only to keep the seven first components when we apply the ICA on any data after the fitting

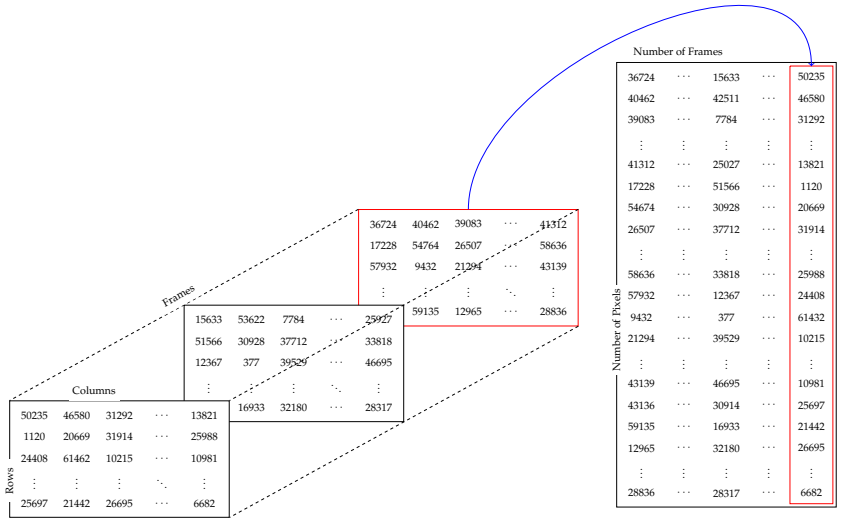

Figure 2. Generation of an overlay matrix from a sequence of images.

step, it returns a matrix of size $7 \times P$. Before computing the metrics, we reshape the output to an array of dimensions $7 \times M \times N$. Note that the position order of the number of components in the dimensions is arbitrary. Then we compute the metrics for each defect and each frame of the output sequence before applying a max-pooling over the frames. Using a mask in which we define both the defect region as well as the sound area for each defect, we computed the scores.

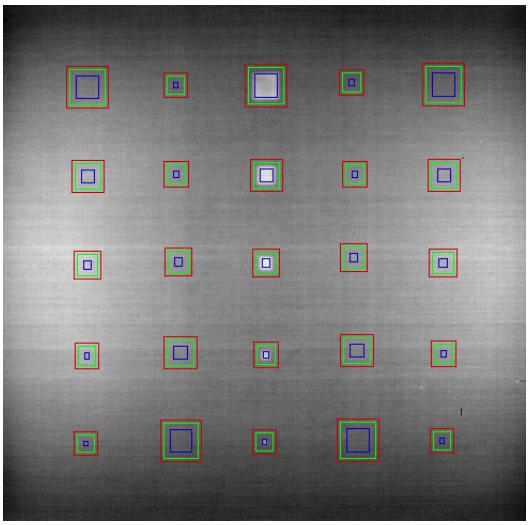

Figure 3. The blue contour represents the defect region, while the region between the green an red contours is our sound area.

Thus we only keep for each defect the best scores. Also note that each algorithm we used has a different set of hyper-parameters. We the prior values of these algorithm allows a computation in a reasonable time, i.e. within 20 minutes we try to tune them. In the next section, we introduce the metric we use for assessing the quality of the different methods we investigated.

2.3. Metrics

To evaluate the proposed works, we choose several metrics to highlight their robustness to different features. The first metric is quite well-known in Infrared Non-

Destructive Testing (IRNDT): it is the Signal to Noise Ratio (SNR). This metric is prevalent in IRNDT due to its ability to provide information about the contrast in the image. Often, thermal or component images are noisy, which can significantly influence this metric. Many formulations of the SNR have been proposed; in this study, we used the formulation proposed by Usamentiaga [31].

$$SNR(roi_s, roi_n) = \frac{|\mu_s - \mu_n|}{\sqrt{\frac{(\sigma_s^2 + \sigma_n^2)}{2}}} \quad (3)$$

The next section introduces the different results we computed for this study.

3. Results

For each experiment we made, we reported the SNR scores obtained by each method for each defect in tables 1 and 2. In figures 4 and 6, we can see for each defect size the SNR scores obtained by each method in the function of the depth. Figures 5 and 7 show for the different depths the SNR score obtained by the different methods in function of the surface of the defects.

Table 1. Maximum SNR values for the different defects, for each method at the frequency of 120 Hz.

Method	Depth (mm) \Lateral size (mm)	3	5	7	10	15
PCT	0.2	3.76	10.53	12.13	15.56	8.55
	0.4	1.63	9.66	3.56	8.41	10.33
	0.6	2.68	6.93	7.44	7.99	8.63
	0.8	2.20	4.39	6.04	8.38	6.25
	1	0.51	3.00	4.10	6.02	6.09
PPT	0.2	3.42	8.33	11.39	11.97	7.92
	0.4	1.50	7.15	3.76	7.79	7.74
	0.6	2.37	6.52	6.38	7.21	6.82
	0.8	1.92	3.77	5.32	7.63	5.71
	1	1.18	2.19	2.95	5.10	5.53
Fast-ICA	0.2	3.45	12.94	10.18	13.32	10.11
	0.4	1.71	7.96	3.05	9.04	9.63
	0.6	2.27	4.92	5.28	5.07	5
	0.8	1.01	3.02	4.94	6.02	4.83
	1	0.47	2.57	3.83	5.52	5.53
Infomax-ICA	0.2	3.56	10.50	11.20	14.18	9.13
	0.4	1.57	9.37	3.57	8.14	10.23
	0.6	2.52	6.77	6.90	8.00	6.73
	0.8	1.76	4.00	5.01	6.97	5.42
	1	0.52	2.24	3.29	4.61	4.73
trust-region-ICA	0.2	3.55	10.23	11.00	15.62	8.63
	0.4	1.64	8.16	3.55	8.10	8.02
	0.6	2.46	6.64	7.04	7.84	6.38
	0.8	1.94	3.83	5.65	7.30	5.99
	1	0.55	2.41	3.45	5.35	5.34
Quasi-newton-ICA	0.2	3.56	10.50	11.20	14.18	9.13
	0.4	1.57	9.37	3.57	8.14	10.23
	0.6	2.52	6.77	6.90	8.00	6.73
	0.8	1.76	4.00	5.01	6.97	5.42
	1	0.52	2.24	3.29	4.61	4.73

Table 2. Maximum SNR values for the different defects, for each method, at frequency of 145 Hz.

Method	Depth (mm) \Lateral size (mm)	3	5	7	10	15
PCT	0.2	2.84	6.4	11.97	15.99	11.33
	0.4	3.39	6.33	9.24	10.54	15.55
	0.6	2.37	7.32	7.45	7.15	12.04
	0.8	1.63	4.52	3.47	8.73	10.16
	1	2.14	3.47	3.88	7.82	5.95
PPT	0.2	3.4	6.64	13.07	15.95	9.32
	0.4	3.16	7.16	11.21	10.74	12.79
	0.6	2.12	7.29	7.38	7.69	10.56
	0.8	1.15	4.73	3.08	7.24	8.26
	1	0.87	3.08	3.55	5.89	6.57
Fast-ICA	0.2	2.78	7.28	12.13	16.63	11.46
	0.4	2.96	5.89	11.2	10.06	12.03
	0.6	2.12	7.58	7.71	7.64	10.31
	0.8	1.47	4.65	3.68	9.36	10.84
	1	1.02	2.70	2.78	4.72	4.05
Infomax-ICA	0.2	0.39	0.18	0.40	0.30	0.50
	0.4	0.12	0.25	0.17	0.34	0.40
	0.6	0.16	0.20	0.39	0.20	0.26
	0.8	0.40	0.25	0.28	0.18	0.14
	1	0.22	0.28	0.35	0.10	0.11
trust-region-ICA	0.2	2.84	6.34	11.85	15.82	11.15
	0.4	3.37	6.29	9.27	10.48	15.57
	0.6	2.36	7.31	7.57	7.14	12.05
	0.8	1.61	4.55	3.46	8.75	10.12
	1	2.14	3.46	3.86	7.76	5.95
Quasi-newton-ICA	0.2	0.39	0.18	0.40	0.30	0.50
	0.4	0.12	0.25	0.17	0.34	0.40
	0.6	0.16	0.20	0.39	0.20	0.26
	0.8	0.40	0.25	0.28	0.18	0.14
	1	0.22	0.28	0.35	0.10	0.11

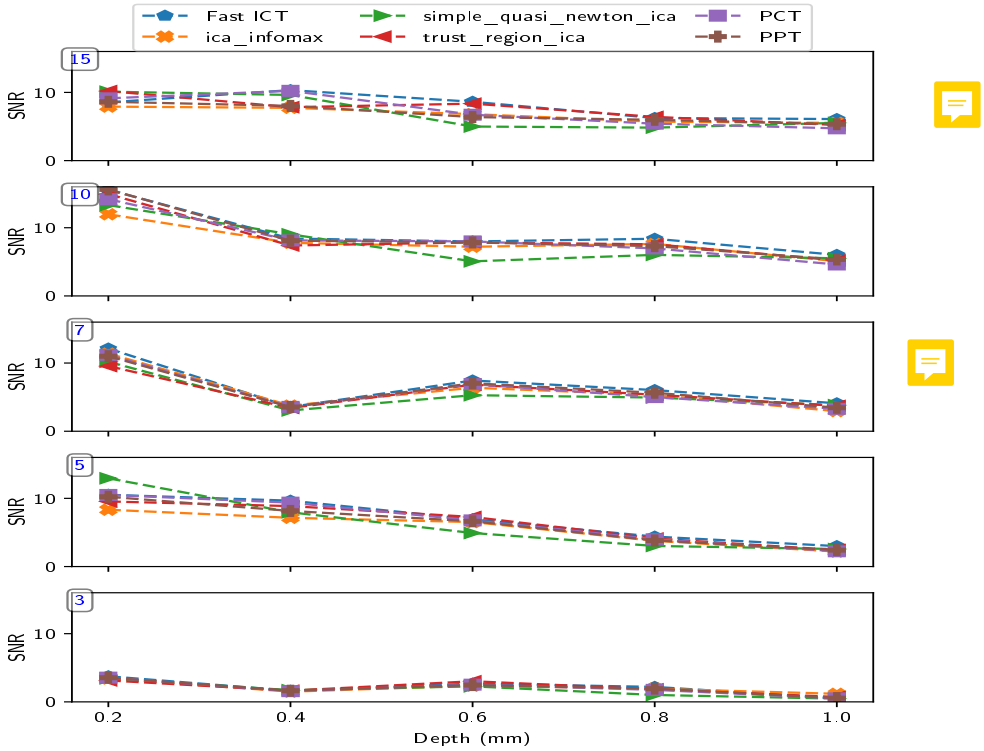

Figure 4. Maximum SNR by defect type as a function of the defect surface for all methods we investigated, which data is acquired at 120 fps.

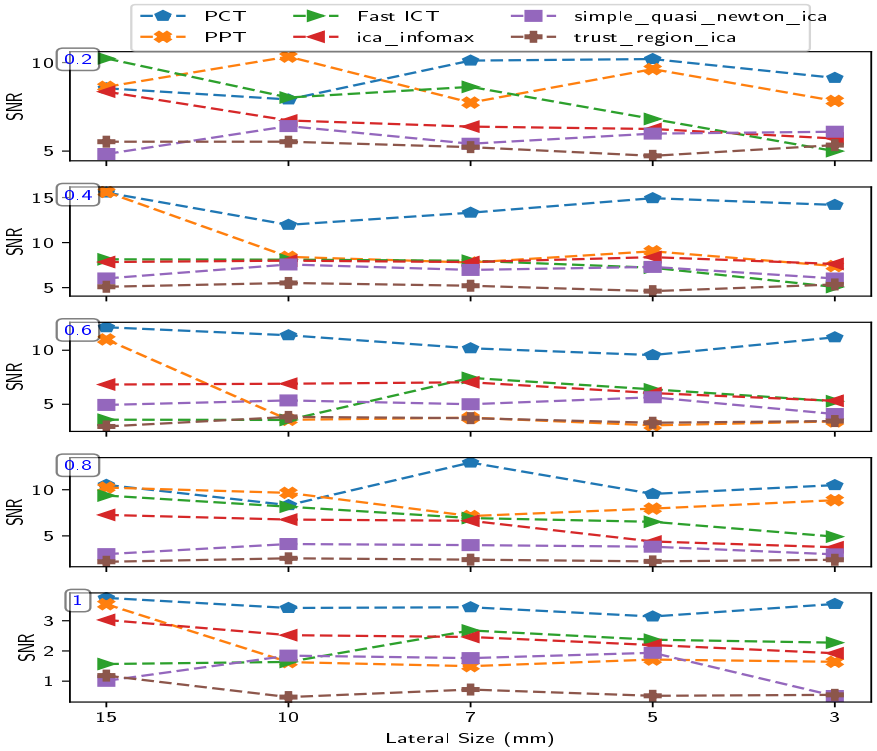

Figure 5. Maximum SNR by defect type as a function of the defect depth for all applied methods , which data is acquired at 120 fps.

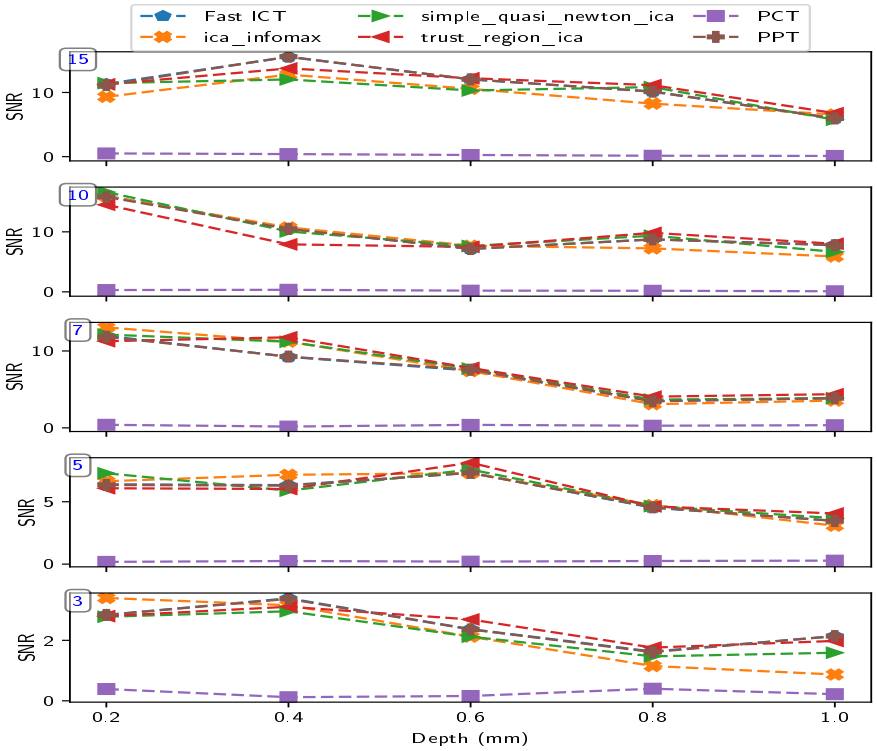

Figure 6. Maximum SNR by defect depth as a function of the defect surface for all applied methods, which data is acquired at 145 fps.

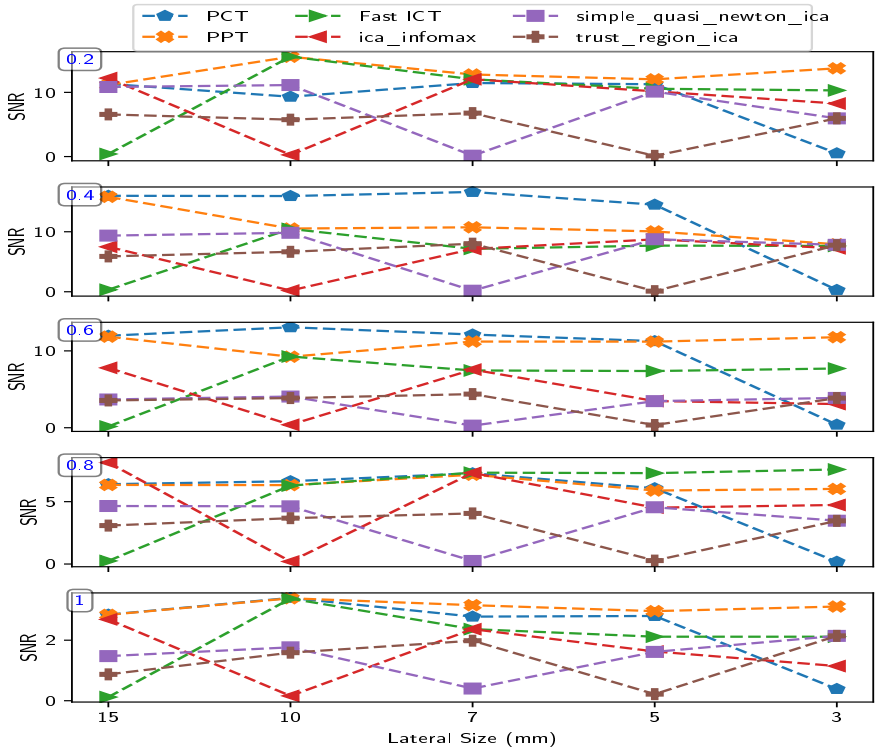

Figure 7. Maximum SNR by defect depth as a function of the defect depth for all applied methods, which data is acquired at 145 fps.

In the next section, we discuss the results we obtained.

4. Discussion

The goal of this study is to evaluate different ICA methods comparatively with state-of-the-art algorithms in order to assess their performance. As one can note in figure 5, the results obtained for the defects with a surface of 15 mm^2 seems unclear. Looking carefully, we can see that depend on the method used; we can categorize three trends. The first trend is followed by the PPT, the quasi-newton ICA, and the Infomax-ICA show a decrease of the SNR score function of the depth. Another trend is followed by the PCT and the Fast-ICA, for which the SNR score increases between the depth of 0.2 mm and 0.4 mm before decreasing for all the other depths. The last trend is only followed by the trust-region ICA, for which we can see a decrease of the SNR score between the depth of 0.2 mm and 0.4 mm, followed by an increase of the score between the depth of 0.4 and 0.6 mm. After 0.6 mm, all the SNR scores decrease with the increase of the depth. Despite the different trends, one can observe that for all the methods, the general trend decrease with depth. For the defects with a surface of 10 mm^2, one can note that the score obtained for the defects located at 0.2 mm from the surface obtained was significantly higher than in the previous plot. We can also see that, like previously observed, the general trend for all the methods is that the SNR score decreases when the depth increase. One can also note that for deeper defects, the Fast-ICA algorithm obtained the best scores. We can also observe that the simple quasi newton ICA is the method that appears to be the most contrasted. From the defects with a surface of 7 mm^2 and lower, we can observe that the smaller is the surface of the defects more similar is the trend regarding the scores obtained for the different methods. In the figure, we can also see that the Fast-ICA outperforms most of the other methods. Another observation is that the smaller is the surface of the defect, the lower is the SNR score, which is expected. Figure 5 shows the scores obtained by the different methods we investigated the function of the defect size for a given depth. At first look, two observations can be made. On the one hand, the deeper is the defect, the lower are the scores, which is expected. On the other hand,

the PCT outperforms all the other methods. One can also note that the infomax-ICA, the simple quasi-newton-ICA, and the region-ICA does not show noticeable variation when the surface of the defect decrease significantly. It is also to note that it does not show a decreasing trend when the surface of the defect decrease. In figure 6, we can see the all the methods outperform the PCT. We can also see that all the methods decrease with the increase of depth. The score related to all the ICA methods close to the scores obtained by the PPT. One can also note that the amplitude of the scores obtained by the different metrics decreases with the size. In 7, one can note that PCT does not perform well on defects the smaller defects. However, PPT performs very well in most situations providing at least similar performances as PCT when not outperforming it. Among the ICA approaches, the Fast-ICA method outperforms all the other methods.
From all these results, we can see that the ICA approaches can provide similar results as state-of-the-art approaches when using to analyze the scores obtained for a surface function of the depth. State-of-the-art approaches outperform ICA's approaches for the analysis of the scores obtained for different sizes at a given depth. Nevertheless, ICA's show a similar trend. As a result, we can conclude that ICA can be used as a replacement for other state-of-the-art methods. In order to provide an extended conclusion regarding the performance of the ICA, we would need further investigation on both noisy data as well as applications data. Among the different methods to compute the ICA, we investigated none of them provided noticeably better results than another on the overall. Comparison with other works such as the work of Rengifo et al. [28] would also provide a clue regarding the performance of the ICA and can possibly also be used with a supervised implementation of the ICA.

5. Conclusions

We studied different implementation of the ICA in order to evaluate their interest for material inspection compaired with state of the art methods sucha as PCT and PPT. We found that if the oftenly ICA underperform state of the art approaches it follows the same trend in every analysis we conducted and therefore more investigations are needed in order to provide an overview of the interest of this method. Among the different implementation of the ICA we use none of them was significantly better than another.

Author Contributions: For research articles with several authors, a short paragraph specifying their individual contributions must be provided. The following statements should be used "Conceptualization, J.F., S.E., C.I., X.M.; methodology, J.F. and S.E.; software, J.F. and S.E.; validation, J.F. and S.E.; formal analysis, J.F. and S.E.; investigation, J.F. and S.E.; data, C.I.; data curation, J.F. and S.E. .

Funding: This research is funded by the NSERC DG program and Canada Research Chair Program (MIVIM Multipolar Infrared Vision Infrarouge Multipolaire).

Conflicts of Interest: The authors declare no conflict of interest.

Abbreviations

The following abbreviations are used in this manuscript:

ICA	Independent Component Analysis
ICT	Independent Component Thermography
PCA	Principal Component Analysis
PCT	Principal Component Thermography
CCIPCA	Candid Covariance free Incremental Principal Component Analysis
CCIPCT	Candid Covariance free Incremental Principal Component Thermography
SPCA	Sparse Principal Component Analysis
SPCT	Sparse Principal Component Thermography
CFRP	Carbon Fiber Reinforced Plastic
PT	Pulsed Thermography
PPT	Pulsed Phase Thermography
LASSO	Least Absolute Shrinkage and Selection Operator
ECT	Eddy Current Testing
PEC	Pulsed Eddy Current
IRNDT	InfraRed Non Destructive Testing
MWIR	Mid-Wave InfraRed
SNR	Signal over Noise Ratio

References

1. Houchin, J.S.; Parulski, K.A. Method and apparatus for pixel non-uniformity correction, 1991. US Patent 5,047,861.
2. Harris, J.G.; Chiang, Y.M. Nonuniformity correction of infrared image sequences using the constant-statistics constraint. *IEEE Transactions on image processing* **1999**, *8*, 1148–1151.
3. Ratliff, B.M.; Hayat, M.M.; Tyo, J.S. Radiometrically accurate scene-based nonuniformity correction for array sensors. *JOSA A* **2003**, *20*, 1890–1899.
4. Perenzoni, M.; Mosconi, D.; Stoppa, D. A 160$\times$ 120-pixel uncooled IR-FPA readout integrated circuit with on-chip non-uniformity compensation. 2010 Proceedings of ESSCIRC. IEEE, 2010, pp. 122–125.
5. Cao, Y.; Tisse, C.L. Single-image-based solution for optics temperature-dependent nonuniformity correction in an uncooled long-wave infrared camera. *Optics letters* **2014**, *39*, 646–648.
6. Maldague, X.; Marinetti, S. Pulse phase infrared thermography. *Journal of applied physics* **1996**, *79*, 2694–2698.
7. Rajic, N. Principal component thermography. Technical report, Defence Science and Technology Organisation Victoria (Australia), 2002.
8. Yousefi, B.; Sfarra, S.; Castanedo, C.I.; Maldague, X.P. Comparative Analysis on Thermal Non-Destructive Testing Imagery Applying Candid Covariance-Free Incremental Principal Component Thermography (CCIPCT). *Infrared Physics & Technology* **2017**, *85*, 163–169.
9. Weng, J.; Zhang, Y.; Hwang, W.S. Candid Covariance-Free Incremental Principal Component Analysis. *IEEE Transactions on Pattern Analysis and Machine Intelligence* **2003**, *25*, 1034–1040.
10. Kompella, V.R.; Luciw, M.; Schmidhuber, J. Incremental slow feature analysis. Twenty-Second International Joint Conference on Artificial Intelligence. Citeseer, 2011.
11. Zou, H.; Hastie, T.; Tibshirani, R. Sparse principal component analysis. *Journal of computational and graphical statistics* **2006**, *15*, 265–286.
12. Yousefi, B.; Sfarra, S.; Sarasini, F.; Castanedo, C.I.; Maldague, X.P. Low-Rank Sparse Principal Component Thermography (Sparse-PCT): Comparative Assessment on Detection of Subsurface Defects. *Infrared Physics & Technology* **2019**, *98*, 278–284.
13. Santosa, F.; Symes, W.W. Linear inversion of band-limited reflection seismograms. *SIAM Journal on Scientific and Statistical Computing* **1986**, *7*, 1307–1330.
14. Comon, P. Independent component analysis, a new concept? *Signal processing* **1994**, *36*, 287–314.
15. Hyvärinen, A.; Oja, E. Independent Component Analysis: Algorithms and Applications. *Neural networks* **2000**, *13*, 411–430.
16. Wang, J.; Wang, C.; Zhang, T.; Zhong, B. Comparison of different independent component analysis algorithms for output-only modal analysis. *Shock and Vibration* **2016**, *2016*.
17. Bell, A.J.; Sejnowski, T.J. An information-maximization approach to blind separation and blind deconvolution. *Neural computation* **1995**, *7*, 1129–1159.
18. Lee, T.W.; Girolami, M.; Sejnowski, T.J. Independent component analysis using an extended infomax algorithm for mixed subgaussian and supergaussian sources. *Neural computation* **1999**, *11*, 417–441.
19. Hyvarinen, A. Fast and robust fixed-point algorithms for independent component analysis. *IEEE transactions on Neural Networks* **1999**, *10*, 626–634.
20. Ablin, P.; Cardoso, J.F.; Gramfort, A. Faster independent component analysis by preconditioning with Hessian approximations. *IEEE Transactions on Signal Processing* **2018**, *66*, 4040–4049.
21. Ablin, P.; Cardoso, J.F.; Gramfort, A. Faster ICA under orthogonal constraint. 2018 IEEE International Conference on Acoustics, Speech and Signal Processing (ICASSP). IEEE, 2018, pp. 4464–4468.

22. Morabito, C.F. Independent Component Analysis and Feature Extraction Techniques for NDT Data. *Materials Evaluation(USA)* **2000**, *58*, 85–92.
23. Morabito, F.; Simone, G. Defect Signal Restoration and Eddy Current Measurments by Independent Component Analysis. *Modelling Measurement and Control a General Physics Electronics and Electrical Engineering* **2001**, *74*, 17–36.
24. Shin, B.H. *Independent Component Analysis for Enhanced Feature Extraction From Non-Destructive Evaluation*; Michigan State University. Department of Electrical and Computer Engineering, 2004.
25. Yang, G.; Tian, G.Y.; Que, P.W.; Chen, T.L. Independent Component Analysis–Based Feature Extraction Technique for Defect Classification Applied for Pulsed Eddy Current NDE. *Research in Nondestructive Evaluation* **2009**, *20*, 230–245.
26. Cheng, L.; Gao, B.; Tian, G.Y.; Woo, W.L.; Berthiau, G. Impact Damage Detection and Identification Using Eddy Current Pulsed Thermography Through Integration of PCA and ICA. *IEEE Sensors Journal* **2014**, *14*, 1655–1663.
27. Wang, F.; Wang, Y.h.; Peng, W.; Ji, J.q.; Liu, J.y.; Xiao, P.; Wang, Y. Independent component analysis enhanced pulse thermography for high silicon oxygen phenolic resin (HSOPR) sheet with subsurface defects. *Infrared Physics & Technology* **2018**, *92*, 345–349.
28. Rengifo, C.J.; Restrepo, A.D.; Nope, S.E. Method of selecting independent components for defect detection in carbon fiber-reinforced polymer sheets via pulsed thermography. *Applied optics* **2018**, *57*, 9746–9754.
29. Pfister, N.; Weichwald, S.; Bühlmann, P.; Schölkopf, B. Robustifying independent component analysis by adjusting for group-wise stationary noise. *Journal of Machine Learning Research* **2019**, *20*, 1–50.
30. Lipshutz, D.; Chklovskii, D.B. Bio-NICA: A biologically inspired single-layer network for Nonnegative Independent Component Analysis. *arXiv preprint arXiv:2010.12632* **2020**.
31. Usamentiaga, R.; Ibarra-Castanedo, C.; Maldague, X. More than Fifty Shades of Grey: Quantitative Characterization of Defects and Interpretation Using SNR and CNR. *Journal of Nondestructive Evaluation* **2018**, *37*, 25.